Journal of Electrical Engineering and Renewable Energies Development (JEERED)
Vol. N°: 2, Issue N°: 1, pp. 36-44, 2026.

Adaptive control of a wind turbine based on a DFIG using a grid-independent rotor supply

Mohammed KENDZI [1], Abdelghani AISSAOUI [2], Dris YOUNES [3], and Abdesselam BOUIRI [4]

[(1)] *Department of Electrical Engineering, Salhi Ahmed Naama University, Naama, Algeria*
[(2)] *Department of Electrical Engineering, Tahri Mohammed Bechar University, Bechar, Algeria*
[(3)] *Department of Electrical Engineering, Tlemcen University, Tlemcen, Algeria*
[(4)] *Department of Electrical Engineering, Ali KAFI University, Tindouf, Algeria*
Email of corresponding author: *kendzi_mohammed@yahoo.com*

Received: 25 February 2026
Accepted for publication: 28 march 2026
Published: 12 April 2026

***Abstract*—**The main objective of this article is to adapt an independent power supply system to optimize the energy production of a wind turbine and thus eliminate power outages on the electrical grid when supplying power to the rotor of a doubly-fed induction generator (DFIG). This system uses a permanent magnet synchronous generator (PMSG) to supply power to the DFIG rotor and offers robust control, comparing PI and sliding mode control methods as a function of varying reference parameters. We begin by presenting the dynamic model of the wind turbine connected to the various generators, followed by the electrical model of the PMSG and DFIG with the control strategy. Next, we explain the theory and mathematical equation of the AC/DC rectifier and the DC/AC inverter. Then, we present the PI controller and the sliding mode control method. Finally, simulation results comparing the PI and sliding mode control methods illustrate and demonstrate the performance and feasibility of this system.

Keywords*—DFIG, wind, PMSG, PI controller, Sliding mode, rectifier AC/DC, inverter DC/AC, control strategy.*

I. INTRODUCTION

To reduce the consumption of traditional fossil energy and environmental pollution, the wind energy is proposed as an optimal solution, as it is a clean and free energy source that has developed over time thanks to technological advances and energy control [1].

In wind turbine systems, the production of electrical energy is undergoing significant development thanks to the emergence of new technologies that allow the operation of new systems called multi-source or multi-generator systems. The choice of the system has become more important as it depends on new criteria related to the different technical and environment problems [2].

Nowadays, the doubly-fed induction generator (DFIG) is employed in wind production system due to its stability in the face of the wind speed variation, reference parameters, maximization of power generation and the competitive price [3] [4] [5].

However, this system remains still incomplete due to the effects of parametric variations, and the lack of production due to the interruption of the electrical network feeding the DFIG rotor.

To solve this problem and ensure the robustness of the production of electrical power, a new system called double generator wind turbine system was proposed, capable of ensuring an uninterrupted power generation. We use the permanent magnet synchronous generator (PMSG) and the doubly-fed induction generator**.** Thus, the maximum power extracted from the wind is converted into mechanical power, then used to produce the electrical energy using two generators: PMSG and DFIG. A part of the power produced by the PMSG is used to feed the DFIG rotor via two static converters: an AC/DC rectifier and a DC/AC inverter.

The power regulation of the DFIG stator is achieved using a PI and a SMC controller. A comparison between the PI and SMC methods is presented to select the controller that best meets the robustness and stability requirements.

The rest of the article is structured as follows: the wind turbine model is presented in section II.. Sections III and IV

© 2026 The Author(s). Licensed under **CC BY-NC-ND 4.0**. Available at http://creativecommons.org/licenses/by-nc-nd/4.0/
e-ISSN 3088-8360, https://web.univ-bechar.dz/jeered

deal with the AC/DC and DC/AC converter models, respectively. Sections V and VI describe the PI and SMC controllers used, respectively. Section VII presents the simulation results. Finally, the conclusions are summarized.

II. Wind Turbine System model

The wind turbine is described in figure 1.

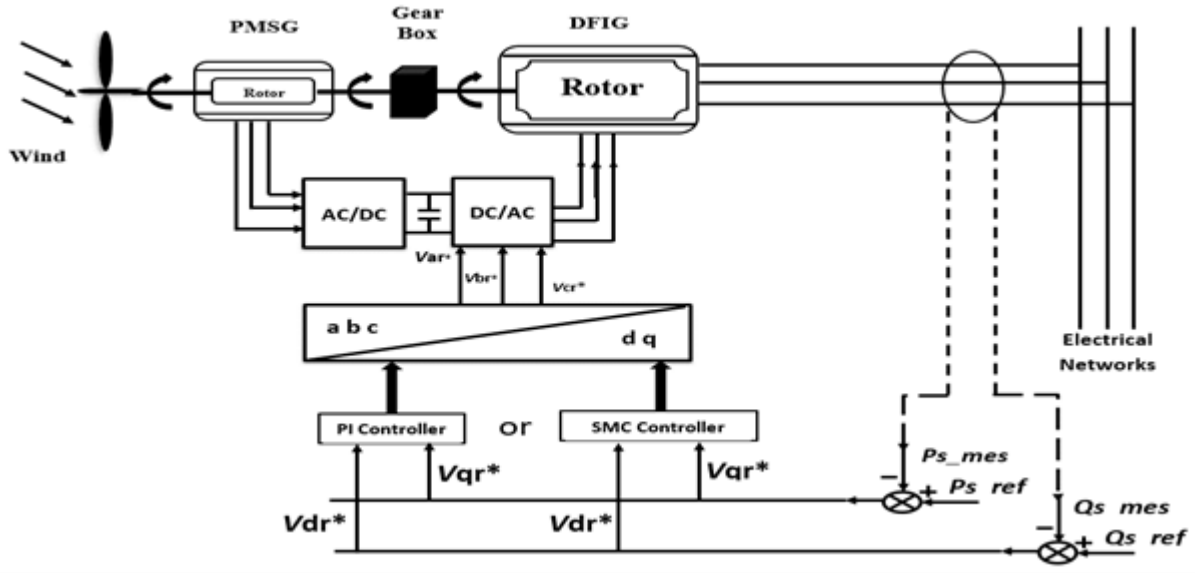

Fig. 1. Wind Turbine system.

A. The wind turbine model:

The wind turbine power equation is [6] :

$$P = \frac{1}{2}\rho S v^3 \tag{1}$$

The available part of this energy that can be captured is: [7]

$$P = \frac{1}{2}\rho C_P S v^3 \tag{2}$$

The equation of the turbine is:

$$\Gamma_m = \Gamma_{em} + f\Omega + J\frac{d\Omega}{dt} \tag{3}$$

B. The PMSG model:

The model of permanent magnet synchronous generator is:

$$\begin{cases} v_{as} = R_s i_{as} + \dfrac{d\varphi_{as}}{dt} \\ v_{bs} = R_s i_{bs} + \dfrac{d\varphi_{bs}}{dt} \\ v_{cs} = R_s i_{cs} + \dfrac{d\varphi_{cs}}{dt} \end{cases} \tag{4}$$

Using the Park model, the permanent magnet synchronous generator equation is given by [8-9] :

$$\begin{cases} v_d = R_s i_d + L_d \dfrac{di_d}{dt} - L_q i_q \omega \\ v_q = R_s i_q + L_q \dfrac{di_q}{dt} + L_d i_d \omega + \phi_f \omega \end{cases} \tag{5}$$

And the electromagnetic torque is given by: [9] [10]

$$\Gamma_{em} = \frac{3}{2} p\left(\left(L_d - L_q\right) i_{ds} i_{qs} + \phi_f i_{qs}\right) \tag{6}$$

C. The DFIG model:

From the Park transformation, the DFIG equations can be written [11]:

$$\begin{cases} v_{ds} = R_s i_{ds} + \dfrac{d}{dt}\phi_{ds} - \omega_s \phi_{qs} \\ v_{qs} = R_s i_{qs} + \dfrac{d}{dt}\phi_{qs} + \omega_s \phi_{ds} \\ v_{dr} = R_r i_{dr} + \dfrac{d}{dt}\phi_{dr} - \left(\omega_s - \omega_r\right)\phi_{qr} \\ v_{qr} = R_r i_{qr} + \dfrac{d}{dt}\phi_{qr} + \left(\omega_s - \omega_r\right)\phi_{dr} \end{cases} \tag{7}$$

$$\begin{cases} \phi_{ds} = L_s i_{ds} + M_{sr} i_{dr} \\ \phi_{qs} = L_s i_{qs} + M_{sr} i_{qr} \\ \phi_{dr} = L_r i_{dr} + M_{sr} i_{ds} \\ \phi_{qr} = L_r i_{qr} + M_{sr} i_{qs} \end{cases} \tag{8}$$

$$\Gamma_{em} = p\frac{M_{sr}}{L_s}\left(\phi_{qs} i_{dr} - \phi_{ds} i_{qr}\right) \tag{9}$$

D. The DFIG control strategy:

From Park transformation, the active and reactive powers are written as follows [10] [11]:

$$\begin{cases} P_s = V_{ds} i_{ds} + V_{qs} i_{qs} \\ Q_s = V_{qs} i_{ds} - V_{ds} i_{qs} \end{cases} \quad (10)$$

And, after using the flux orientation method, we can write:

$$\begin{cases} \phi_{qs} = 0 \ ; \ \phi_{ds} = \phi_s \\ V_{qs} = V_s \ ; \ V_{ds} = 0 \end{cases} \quad (11)$$

Substitutin equation (11) in (10) we have:

$$\begin{cases} P_s = V_{qs} i_{qs} \\ Q_s = V_{qs} i_{ds} \end{cases} \quad (12)$$

By combining (7), (8), and (12), equation (12) becomes:

$$\begin{cases} P_s = -V_s \dfrac{M}{L_s} i_{qr} \\ Q_s = -V_s \dfrac{M}{L_s} i_{dr} + \dfrac{V_s^2}{L_s \omega_s} \end{cases} \quad (13)$$

The equation voltage of the rotor can be expressed by:

$$\begin{cases} v_{qr} = R_r i_{qr} + \delta \dfrac{di_{qr}}{dt} + \omega_g \delta i_{dr} + \dfrac{gMV_s}{L_s} \\ v_{dr} = R_r i_{dr} + \delta \dfrac{di_{dr}}{dt} - \omega_g \delta i_{qr} \end{cases} \quad (14)$$

Where: $\delta = L_r - \dfrac{M^2}{L_s}$ is the leakage factor, and $g = (\omega_s - \omega_r)/\omega_r$ is generator slip.

III. Rectifier Modelisation AC/DC

The AC/DC converter consists of six diodes arranged according to the structure illustrated in the figure 2. The converter is powered by a three-phase voltage system.

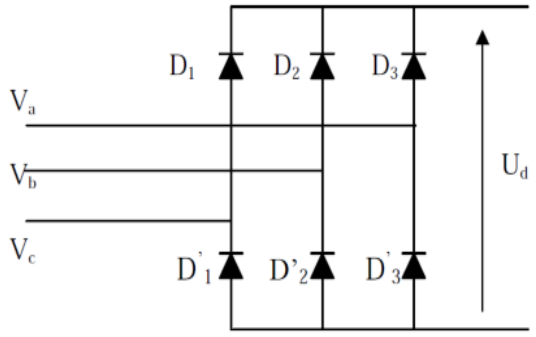

Fig. 2. AC/DC rectifier.

In this rectifier system, we have:

D_i in conduction position, Si: $\begin{cases} V_i = Max\ (V_j) \\ i = 1,2,3 \text{ and } j = 1,2,3 \end{cases}$

D'_i in conduction position, Si: $\begin{cases} V'_i = Min\ (V_j) \\ i = 1,2,3 \text{ and } j = 1,2,3 \end{cases}$

So, the output voltage of this rectifier is given by:

$$U_d = Max(V_j) - Min(V_j); \ j = 1,2,3 \quad (15)$$

IV. Inverter Modelisation DC/AC

The DC/AC converter is presented by its power circuit in figure 3:

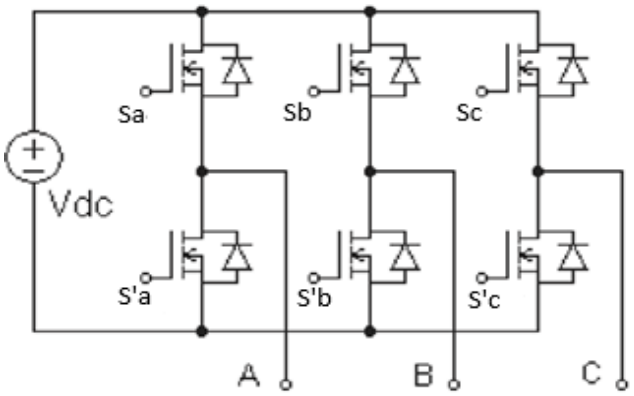

Fig. 3. DC/AC inverter.

We can obtain the inverter output branch voltages as follows:

$$\begin{cases} V_{AN} = S_a \times V_{dc} \\ V_{BN} = S_b \times V_{dc} \\ V_{CN} = S_c \times V_{dc} \end{cases} \quad (16)$$

Where S_a, S_b and S_c design the switches states.

Equation of compound voltages:

$$\begin{cases} V_{AB} = V_{AN} + V_{NB} = V_{AN} - V_{BN} = (S_a - S_b) V_{dc} \\ V_{BC} = V_{BN} + V_{NC} = V_{BN} - V_{CN} = (S_b - S_c) V_{dc} \\ V_{CA} = V_{CN} + V_{NA} = V_{CN} - V_{AN} = (S_c - S_a) V_{dc} \end{cases} \quad (17)$$

Equation of simple voltages:

$$\begin{cases} V_{AN} = \dfrac{1}{3}(2V_{AN} - V_{BN} - V_{CN}) \\ V_{BN} = \dfrac{1}{3}(2V_{BN} - V_{AN} - V_{CN}) \\ V_{CN} = \dfrac{1}{3}(2V_{CN} - V_{AN} - V_{BN}) \end{cases} \quad (18)$$

After the replace of equation 16 in the equation 18, we find:

$$\begin{cases} V_{AN} = \dfrac{1}{3} V_{dc} (2S_a - S_b - S_c) \\ V_{BN} = \dfrac{1}{3} V_{dc} (2S_b - S_a - S_c) \\ V_{CN} = \dfrac{1}{3} V_{dc} (2S_c - S_a - S_b) \end{cases} \quad (19)$$

Finally, the inverter equation are expressed by:

$$\begin{cases} V_{as} = \frac{1}{3} V_{dc} \left(2S_a - S_b - S_c\right) \\ V_{bs} = \frac{1}{3} V_{dc} \left(2S_b - S_a - S_c\right) \\ V_{cs} = \frac{1}{3} V_{dc} \left(2S_c - S_a - S_b\right) \end{cases} \quad (20)$$

V. PI CONTROLLER

In this system, we are interested to control the powers (P_s , Q_s) and the currents (I_{dr} , I_{qr}) by PI controller.

A. Rotor currents control:

Figure 4 shows the rotor currents control by the proportional-integral controller. The simplified transfer function obtained from equation (14) corresponds to a first-order system.

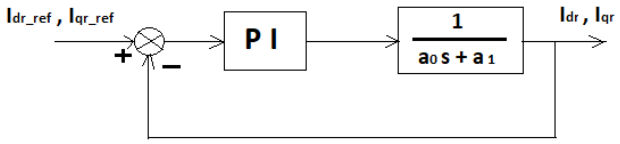

Fig. 4. Transfer function of a PI controller

The PI transfer function controller:

$$C_s = K_p + \frac{K_i}{s} \quad (21)$$

Therefore, the open-loop transfer function is given by:

$$T(s) = \frac{K_p\, s + K_i}{a_0\, s^2 + a_1\, s} \quad (22)$$

Where $a_0 = \delta$ and $a_1 = R_r$

And the closed-loop transfer function is:

$$F(s) = \frac{T(s)}{1+T(s)} = \frac{1+\tau\, s}{\frac{a_0}{K_i} s^2 + \left(\tau + \frac{a_1}{K_i}\right) s + 1} \quad (23)$$

Where: $\tau = \frac{K_p}{K_i}$

B. Active and reactive power control:

The Figure 5 illustrated the control loop of powers (P_s , Q_s) using PI regulator.

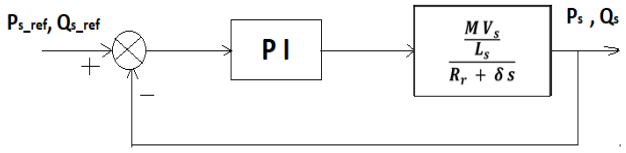

Fig. 5. Transfer function of active and reactive power PI controller

The PI transfer function controller is:

$$C(s) = \frac{1+s\, T_n}{s\, T_i} \quad (24)$$

Where T_i *and* T_n are respectively the constant time of the integration correlation and the integration time constant.

The open-loop transfer function:

$$F_0(s) = \frac{1+s\, T_n}{s\, T_i} \frac{\frac{M\, V_S}{L_S}}{R_r + \delta\ s} \quad (25)$$

In a closed loop, we obtain the following transfer function:

$$F_F(s) = \frac{F_0(s)}{1+F_0(s)} = \frac{\frac{1+s\, T_n}{s\, T_i} \frac{\frac{M\, V_S}{L_S}}{R_r + \delta\ s}}{1 + \frac{1+s\, T_n}{s\, T_i} \frac{\frac{M\, V_S}{L_S}}{R_r + \delta\ s}}$$

$$F_F(s) = \frac{M\, V_S}{T_i \delta L_S} \frac{1+T_n s}{s^2 + \left(\frac{R_r}{\delta} + \frac{T_n M\, V_S}{T_i \delta L_S}\right) s + \frac{M\, V_S}{T_i \delta L_S}}$$

$$F_F(s) == K_r \frac{1+T_n s}{s^2 + \left(\frac{R_r}{\delta} + \frac{T_n\, M\, V_S}{T_i\, \delta\, L_S}\right) s + \frac{M\ V_S}{T_i\, \delta\, L_S}} \quad (26)$$

Where: $K_r = \frac{M\ V_S}{T_i\ \delta\ L_S}$

VI. SLIDING MODE CONTROL

The Sliding mode control (SMC) is a robust nonlinear control technique. It stabilizes the dynamic behavior of the controlled system in the presence of uncertainties; it is simple and robust to disturbances. The SMC comprises three stages. [12]:

- The fist step consists in choosing sliding surface:

$$\begin{cases} S(X) = \left(\frac{d}{dt} + \lambda_c\right)^{n-1} e \\ e = X^d - X \end{cases} \quad (27)$$

With:

$$\begin{cases} X = \left[x, \dot{x}, \ldots, x^{n-1}\right]^T \\ X^d = \left[x^d, \dot{x}^d, \ddot{x}^d, \ldots\right]^T \end{cases} \quad (28)$$

- The second step is to guarantee the conditions for the convergence and the stability of the system:

$$\left(S(X)\right)\left(\dot{S}(X)\right) \le 0 \quad (29)$$

- The third step the law control design:

$$u = u^{eq} + u^n \quad (30)$$

Where u^n is the switching term, u^{eq} is the equivalent control.

We apply sliding mode control theory to control the powers (P_s , Q_s). [12]

A. Active power control

To control the power, we take n = 1, the expression of the control surface of the active power has the form:

$$S(P) = \left(P_s^{ref} - P_s \right) \quad (31)$$

We define:

$$\dot{S}(P) = \left(\dot{P}_s^{ref} - \dot{P}_s \right) \quad (32)$$

We substitute equation 13 in 32:

$$\dot{S}(P) = \left(\dot{P}_s^{ref} + V_s \frac{M}{L_s} \dot{i}_{qr} \right) \quad (33)$$

We use equations 14 and 33, We obtain:

$$\dot{S}(P) = \left(\dot{P}_s^{ref} + V_s \frac{M}{L_s L_r \sigma} \left(v_{qr} - R_r i_{qr} \right) \right) \quad (34)$$

With: $\sigma = 1 - \frac{M^2}{L_r L_s}$

Replacing the expression of v_{qr} with $v_{qr}^{eq} + v_{qr}^{n}$ the equation 34 become:

$$\dot{S}(P) = \left(\dot{P}_s^{ref} + V_s \frac{M}{L_s L_r \sigma} \left(\left(v_{qr}^{eq} + v_{qr}^{n} \right) - R_r i_{qr} \right) \right) \quad (35)$$

In steady state and in the slip mode, we have:

$$S(P) = 0 \ , \ \dot{S}(P) = 0 \ , \ v_{qr}^{n} = 0 \quad (36)$$

From the equation 35 and 36, the equivalent term command is written:

$$v_{qr}^{eq} = -\dot{P}_s^{ref} \frac{\sigma L_s L_r}{V_s M} + R_r i_{qr} \quad (37)$$

In convergence mode, using the condition $S(P)\dot{S}(P) \le 0$ we set:

$$\dot{S}(P) = -V_s \frac{M}{\sigma L_s L_r} v_{qr}^{n} \quad (38)$$

The switching term is defined by:

$$v_{qr}^{n} = K v_{qr} sign\left(S(P) \right) \quad (39)$$

Where Kv_{qr} is a positive parameter.

B. Control of reactive power

To control the power, we take n = 1, the expression of the control surface of the reactive power has the form:

$$S(Q) = \left(Q_s^{ref} - Q_s \right) \quad (40)$$

We define:

$$\dot{S}(Q) = \left(\dot{Q}_s^{ref} - \dot{Q}_s \right) \quad (41)$$

We substitute equation 13 in 41:

$$\dot{S}(Q) = \left(\dot{Q}_s^{ref} - \left(-V_s \frac{M}{L_s} \dot{i}_{dr} \right) \right) \quad (42)$$

We use equations 14 and 43, We obtain:

$$\dot{S}(Q) = \left(\dot{Q}_s^{ref} + V_s \frac{M}{L_s L_r \sigma} \left(v_{dr} - R_r i_{dr} \right) \right) \quad (43)$$

Replacing the expression of v_{dr} with: $v_{dr}^{eq} + v_{dr}^{n}$ the equation 43 become:

$$\dot{S}(Q) = \left(\dot{Q}_s^{ref} + V_s \frac{M}{L_s L_r \sigma} \left(\left(v_{dr}^{eq} + v_{dr}^{n} \right) - R_r i_{dr} \right) \right) \quad (44)$$

In steady state and in the slip mode, we have:

$$S(Q) = 0 \ , \ \dot{S}(Q) = 0 \ , \ v_{dr}^{n} = 0 \quad (45)$$

From the equation 35 and 36, the equivalent term command is written:

$$v_{dr}^{eq} = -\dot{Q}_s^{ref} \frac{\sigma L_s L_r}{V_s M} + R_r i_{dr} \quad (46)$$

In convergence mode, using the condition $S(P)\dot{S}(P) \le 0$ we set:

$$\dot{S}(Q) = -V_s \frac{M}{\sigma L_s L_r} v_{dr}^{n} \quad (47)$$

Therefore, the switching term is given by:

$$v_{dr}^{n} = K v_{dr} sign\left(S(Q) \right) \quad (48)$$

Where Kv_{dr} is a positive parameter.

VII. Implementation and results

Active and reactive power control is achieved using a PI and a sliding mode controller. The Blocks diagram of PMSG-DFIG/PI and PMSG-DFIG/SMC system are presented respectively in Figure 6 and Figure 7.

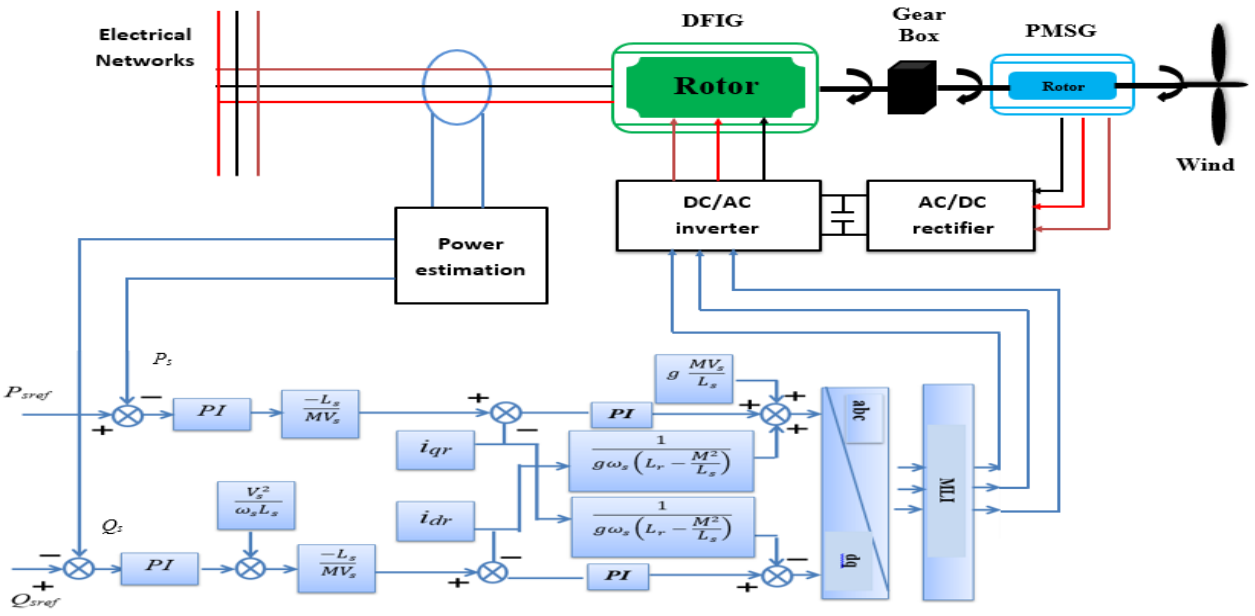

Fig. 6. PMSG-DFIG/PI control system.

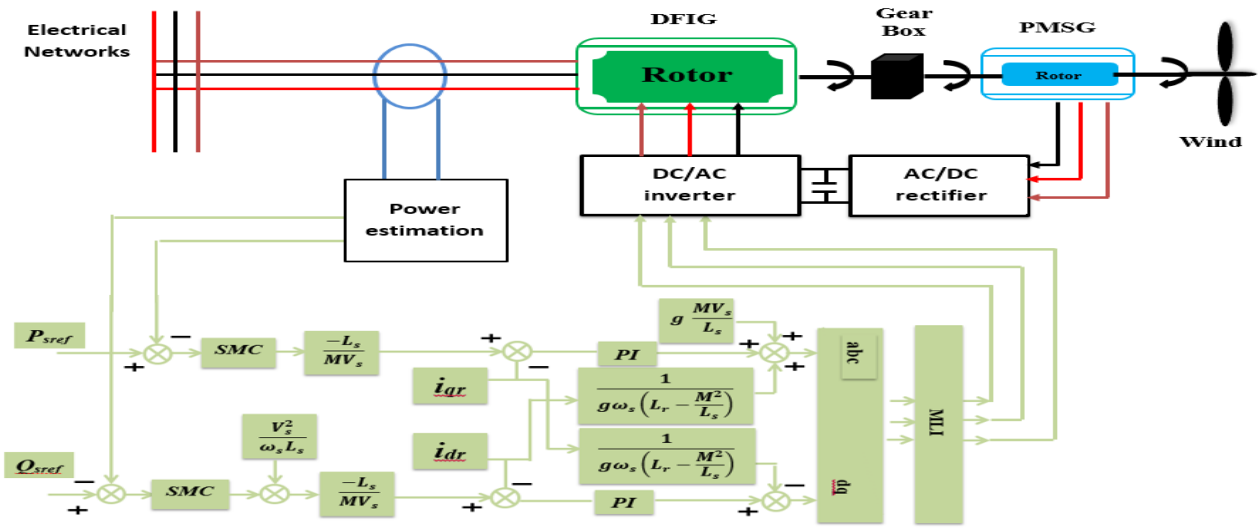

Fig. 7. PMSG-DFIG/SMC control system.

Tin this section the systems in figures 6 and 7 are simulated using the Matlab-Simulink environment. The control of a dual-generator wind system (PMSG-DFIG) aims to improve performance and stability in the face of variations in the references.

The variation in mechanical speed is illustrated in Figure 8 with different values (50, 90, 40, and 125 rad/s).

In figures 9 and 10, we have the powers Ps and Qs produced by the PMSG resulting from the wind speed and used to supply the DFIG rotor.

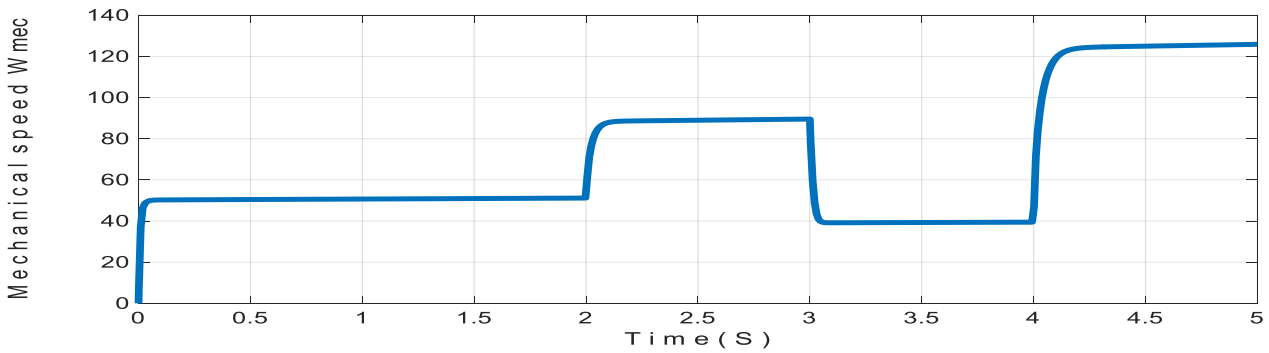

Fig. 8. Mechanical speed variation.

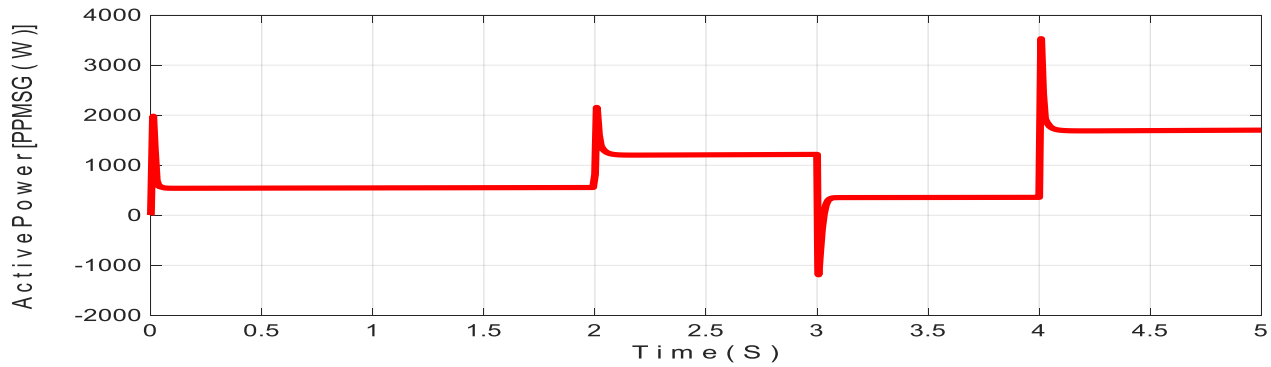

Fig. 9. Active power supplying the DFIG rotor and generated by the PMSG.

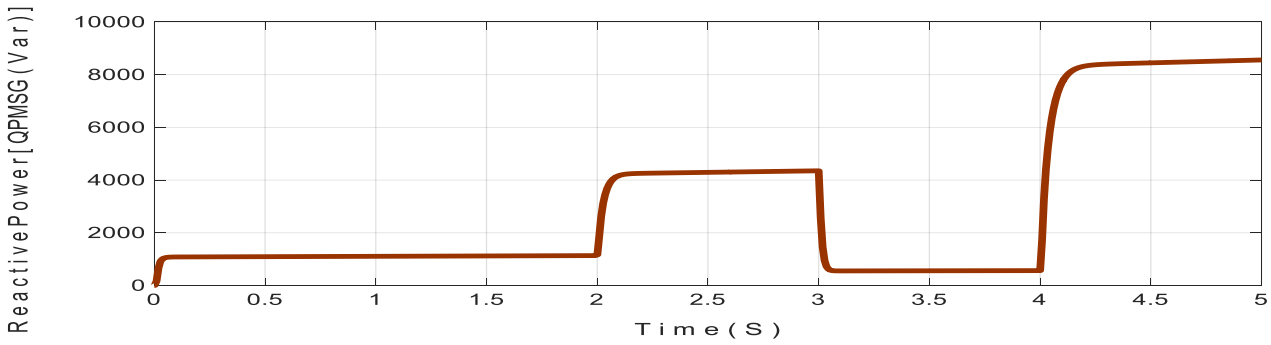

Fig. 10. Active power supplying the DFIG rotor and generated by the PMSG.

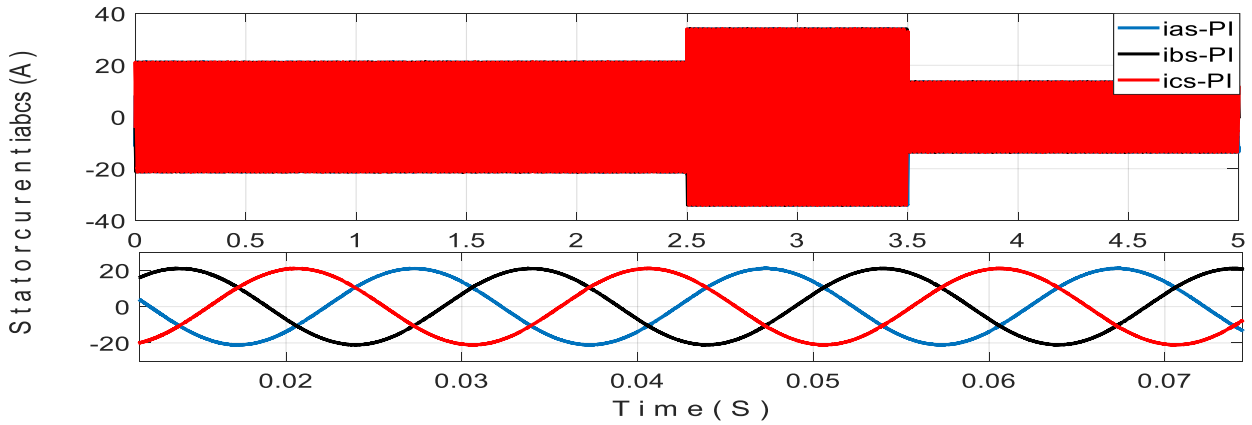

Fig. 11. Stator current of DFIG generator controlled by PI controller.

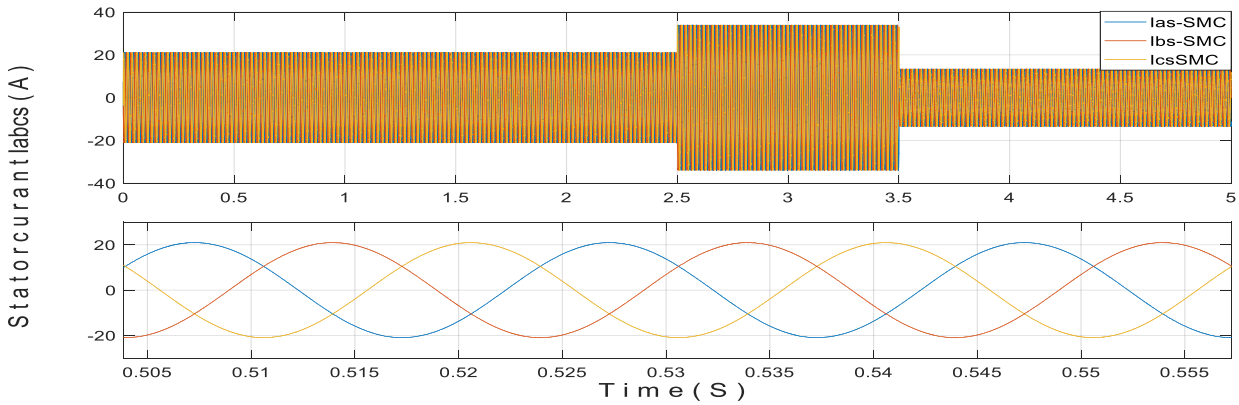

Fig. 12. Stator current of DFIG generator controlled by SMC controller.

Figures 11 and 12 show the evolution of the stator current generated on the grid by the system over time as a function of the variation of the active and reactive power reference.

For system robustness, we carried out a comparison between the regulation of the current at the output of the DFIG by two modes of regulation (PI regulation and sliding mode) as shown in figure 13.

We therefore observe good robustness of the SMC regulation of the generated stator current compared to the PI regulation..

Figures 14 and 15 show the regulation of the DFIG's Ps and Qs powers over time as a function of the variation of the active and reactive power reference. A better system response is observed with an SMC controller than with a PI controller for controlling the powers P_s and Q_s generated by DFIG.

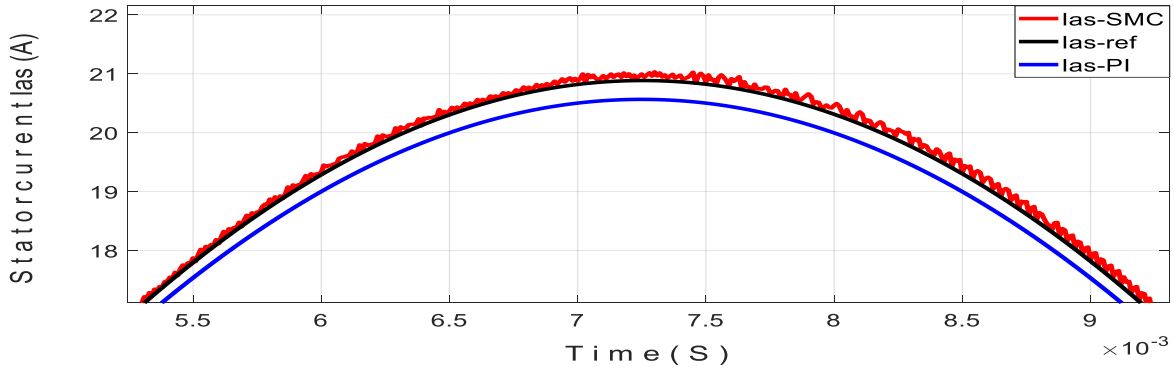

Fig. 13. Comparison between PI and SMC control in zooming mode.

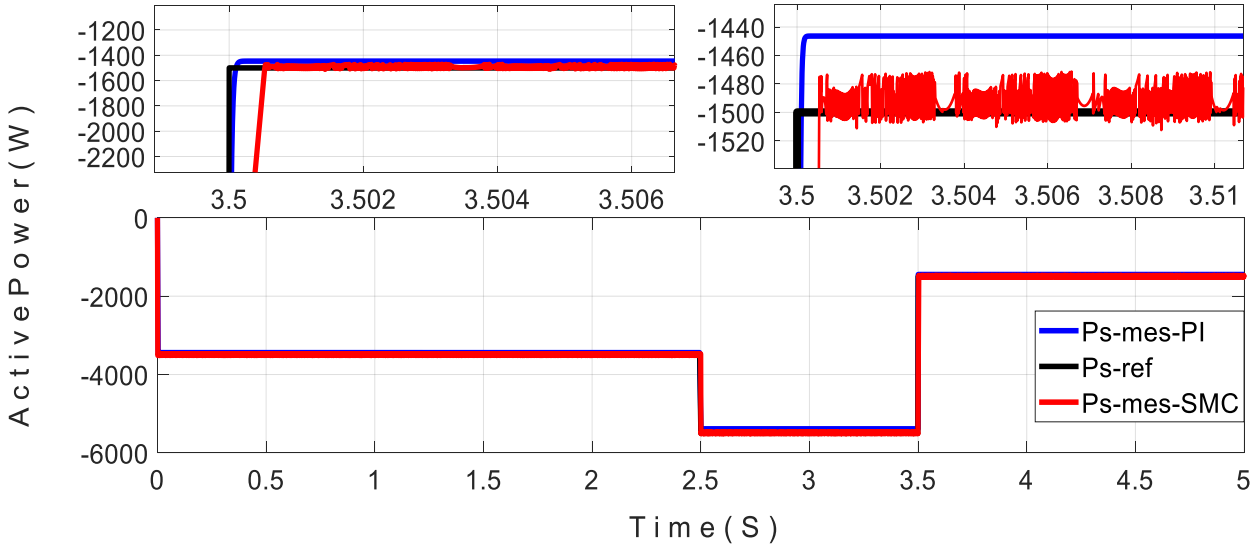

Fig. 14. Comparison between PI and SMC in the active powers adaptation

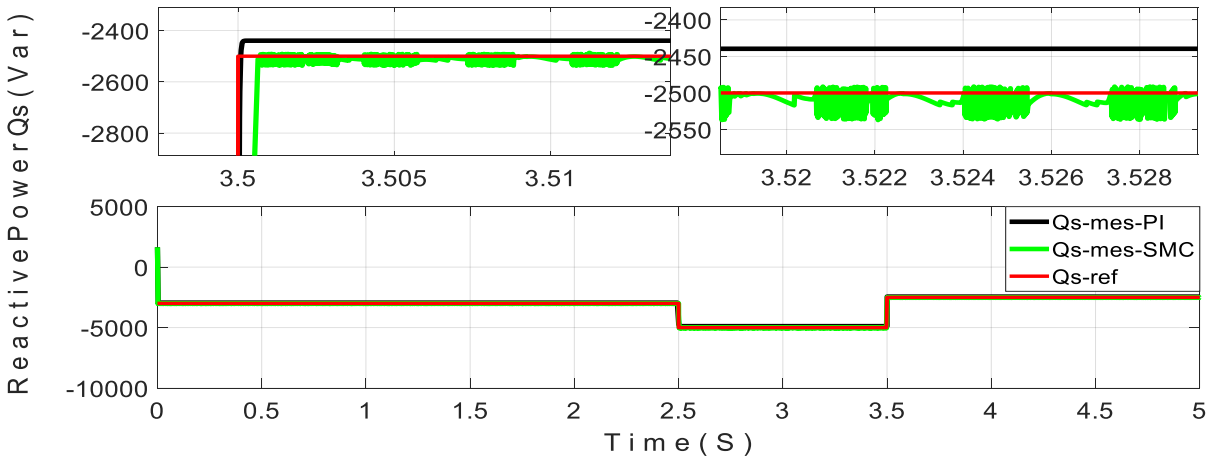

Fig. 15. Comparison between PI and SMC in the reactive powers adaptation

VIII. CONCLUSION

The principle objective of this article, is to establish an independent power supply system, to eliminate the problem of power outages in electrical networks when supplying the rotor of a DFIG using a PMSG, and elaborate a robust control, responding to stability criteria and desired performances, for wind system in variation of system reference parameters.

So firstly, the double generator wind turbine system (PMSG-DFIG) is presented using PMSG to feed a DFIG rotor.

Secondly, an AC/DC rectifier and a DC/AC inverter are used to connect the PMSG stator and the DFIG rotor. The P_s and Q_s powers at the output of the PMSG are used to power the DFIG rotor.

Next, the control of P_s and Q_s are realized by the PI and SMC methods.

The results obtained by simulation show that the system composed of two generators is stable, as well as the dynamic performance and robustness of the SMC control method. compared to the PI controller in an adaptive production system

Finally, this paper concludes that this system (double generator wind turbine system (PMSG-DFIG)) has a good stability and high robustness in the presence of variations in the reference parameter system and interruptions electrical network.

REFERENCES

[1] A. Kumar, B. Pandey, M. Zafar U. Khan, "Wind Energy: A Review Paper", Gyancity Journal of Engineering and Technology, Vol.4, No.2, July 2018, pp.29-37, DOI: 10.21058/gjet.2018.42004

[2] B. Su, T. Guo, Md. M. Alam, "A review of wind energy harvesting technology: Civil engineering resource, theory, optimization, and application", Applied Energy, Vol. 389, 1 July 2025, Art. Numb. 125771, https://doi.org/10.1016/j.apenergy.2025.125771

[3] K. Thota, S. Velpula, V. Basetti, "A scientometric analysis on DFIG-based wind energy conversion system research trends", Discover Applied Sciences, Vol. **7**, Art Numb. 7, 2025. https://doi.org/10.1007/s42452-024-06373-4

[4] A. E. Elngar, A. S. Sabik, A. H. Adel, A. S. Nada, "Comparative Performance Evaluation of Wind Energy Systems Using Doubly Fed Induction Generator and Permanent Magnet Synchronous Generator", *Wind*, Vol. *5, N°* 4, Art. Numb. 31. (2025). https://doi.org/10.3390/wind5040031

[5] S. Karimi, A. Gaillard, P. Poure and S. Saadate, "FPGA-Based Real-Time Power Converter Failure Diagnosis for Wind Energy Conversion Systems," in *IEEE Transactions on Industrial Electronics*, vol. 55, no. 12, pp. 4299-4308, Dec. 2008, doi: 10.1109/TIE.2008.2005244.

[6] B. Hamane, M. L. Doumbia, M. Bouhamida, And M. Benghanem, "Control of wind turbine based on DFIG using fuzzy-PI and sliding mode controllers, " Ninth International Conference on Ecological Vehicles and Renewable Energies (EVER), DOI: 10.1109/EVER.2014.6844060, 2014.

[7] M. Kendzi, A. Aissaoui, M. Abid, and A. Tahour, "Control of the photoelectric generator for used in feeding of the independent wind turbine system, " International Journal of Power Electronics and Drive System (IJPEDS), vol. 10, No. 3, pp. 1613-1627, Septomber 2019. DOI: 10.11591/ijpeds.v10.i3.pp1613-1627

[8] A. Harrouz, I. Colak, and K. Kayisili, "Control Strategy of PMSG Generator in Small Wind Turbine System , " Algerian Journal of Renewable Energy and Sustainable Development , vol. 4, pp. 69-83, 2022.

[9] S. R. Zine, B. Mazari, M. A. Bouzid, and Y. Mihoub, "Synergistic and sliding mode controls of wind energy conversion system," International Review on Modelling and Simulations (I.RE.MO.S.), vol. 8, No. 6, pp. 610-619, 2015. DOI: https://doi.org/10.15866/iremos.v8i6.8022

[10] R. A. Mohamed, M. A. Mossa, A. El-Gaafary, (2023). Performance Enhancement of a Variable Speed Permanent Magnet Synchronous Generator Used for Renewable Energy Application. *International Journal of Robotics and Control Systems,* vol. 3, No. 3, pp. 530-560. doi:https://doi.org/10.31763/ijrcs.v3i3.1031

[11] M. Kendzi, and A. Aissaoui, " Comparison between the MIT rule and fuzzy logic controller to adapting the power generated by a doubly fed induction generator integrated in a wind system." 10th IEEE International Conference on Smart Grid, June 27-29, Istanbul, TURKEY, 2022. DOI:10.1109/icSmartGrid55722.2022.9848520,

[12] T. T Tuyen, J.Yang, L. Liao, N. G. M. Thao, " Recent Advances in Sliding Mode Control Techniques for Permanent Magnet Synchronous Motor Drives" . *Electronics*. Vol. 14, N° 19, Art. Numb. 3933, 2025, https://doi.org/10.3390/electronics14193933